
RoSA: ACCURATE PARAMETER-EFFICIENT FINE-TUNING VIA ROBUST ADAPTATION

Mahdi Nikdan*
 IST Austria
 mahdi.nikdan@ist.ac.at

Soroush Tabesh*
 IST Austria
 soroush.tabesh@ist.ac.at

Dan Alistarh
 IST Austria & Neural Magic
 dan.alistarh@ist.ac.at

ABSTRACT

We investigate parameter-efficient fine-tuning (PEFT) methods that can provide good accuracy under limited computational and memory budgets in the context of large language models (LLMs). We present a new PEFT method called Robust Adaptation (RoSA) inspired by robust principal component analysis (PCA) that jointly trains *low-rank* and *highly-sparse* components on top of a set of fixed pretrained weights to efficiently approximate the performance of a full-fine-tuning (FFT) solution. Across a series of challenging generative tasks such as grade-school math and SQL query generation, which require fine-tuning for good performance, we show that RoSA outperforms both LoRA and pure sparse fine-tuning, at the same parameter budget. We provide system support for RoSA to complement the training algorithm, specifically in the form of sparse GPU kernels which enable memory- and computationally-efficient training. Our code will be made available at <https://github.com/IST-DASLab/RoSA>.

1 Introduction

The advances brought about by state-of-the-art large language models (LLMs) have been accompanied by extremely large computational and memory costs, especially for training such models from scratch. In this context, fine-tuning LLMs using a limited amount of data has become an effective and popular approach to improve LLM performance on specific tasks, e.g. [WBZ⁺21, OWJ⁺22, WKM⁺22, LTM⁺22], or adapt LLMs to better fit expected user behavior [ABC⁺21, BJJ⁺22]. Yet, full fine-tuning of all LLM parameters (FFT), can be extremely expensive, especially in terms of memory cost, rendering this process prohibitive for end users.²

Parameter-Efficient Fine-Tuning (PEFT) methods address this issue, by allowing users to optimize only over a restricted set of parameters, relative to the original model. On the one hand, this allows partial accuracy recovery relative to FFT, at a fraction of its computational and memory cost. An extremely popular recent instance of PEFT in the context of LLMs is given by the Low-Rank Adaptation (LoRA) family of methods [HSW⁺21], which train low-rank “adapter” layers for a selection of the model layers. LoRA methods are based on the intuition that the fine-tuning updates of pre-trained LLMs have low “intrinsic rank” during specialization to a sub-task, which allow these updates to be well-approximated by adapters. Besides memory and computational cost reductions, low-rank adaptation also has the advantage of implicit regularization, which can lead to more stable training, and reduce the need for hyper-parameter search.

One key weakness of LoRA-type methods is the fact that they can fail to recover accuracy for “harder” fine-tuning tasks, relative to FFT. This accuracy gap, illustrated in Figure 1a, appears more likely to occur when the target tasks is more complex, such as the case for mathematical reasoning or coding tasks. It is therefore still an open question whether there exist PEFT methods which combine the good practical performance and ease-of-use of LoRA-type methods with the high accuracy of FFT.

Contribution. In this paper, we take a step towards addressing this question, by proposing a new PEFT method called **RobuSt Adaptation (RoSA)**. RoSA has similar computational and memory cost relative to LoRA-type methods,

*These authors contributed equally.

²For example, full fine-tuning of a popular LLaMA2 model [TLI⁺23] with 70B parameters requires more than 8 NVIDIA A100 GPUs, with 80GB of memory each.

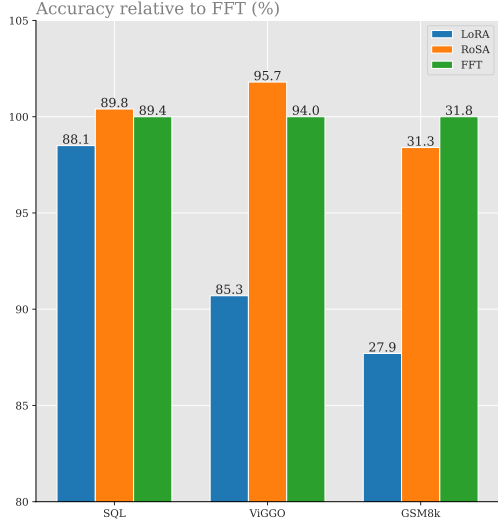


Figure 1(a): Comparison of the highest achieved accuracy by a single-epoch adaptation using various methods across three datasets on LLaMA2-7B, taken from our main experiments in Table 1. Each bar shows the percentage of accuracy relative to the accuracy achieved by FFT, and the numbers on top of the bars indicate the absolute value of accuracy.

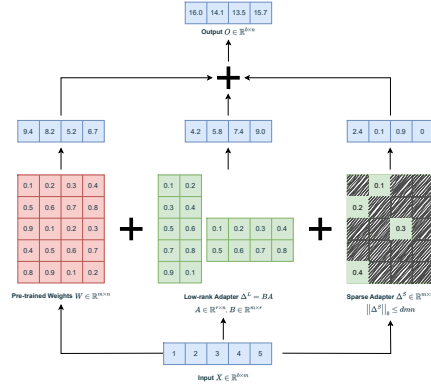


Figure 1(b): Illustration of Robust Adaptation (RoSA) applied to a single FC layer: In this instance, the weight matrix is of dimensions 5×4 and the batch size is 1. The low-rank adapter has a rank of 2, and the sparse adapter has a density of 20%. Trainable parameters are depicted in green, while red indicates parameters that remain frozen.

but is significantly more accurate at similar parameter and computational budgets, while being easy to use and tune. Specifically, in practical experiments RoSA essentially matches the accuracy of full fine-tuning, while offering stable convergence and relatively simple hyper-parameter tuning. We complement these algorithmic observations with a practical implementation, showing that RoSA preserves the memory advantage of LoRA-type methods.

The motivation behind RoSA comes by revisiting the low “intrinsic rank” assumption that is the basis for the LoRA family of methods. Specifically, our investigation across several tasks shows that, while the FFT update can indeed be well approximated by a low-rank matrix, one can obtain a significantly better fit via a *low-rank plus sparse matrix*, especially in the case of more complex tasks. Intuitively, the latter representation is better suited to matching outlier components which can cause a significant fraction of the compression error in the context of LLMs [DLBZ22, DSE⁺23]. This observation provides a connection to the area of robust principal component analysis (robust PCA) [CLMW11], which postulates that matrices arising from a noisy series of measurements can often be approximated as a sum between a low-rank component and a sparse one, investigating algorithms for recovering such matrices. Starting from the hypothesis that the sum of gradient updates corresponding to FFT can be seen as an instance of robust PCA, we investigate methods for recovering such a sparse plus low-rank representation during training.

Concretely, our proposed scheme trains *two adapters*: a standard low-rank adapter, complemented by a sparse adapter. Both of these adapters are trained “in parallel” relative to the original pre-trained weights, and the challenge is to find a co-training mechanism which yields stable convergence. Building on prior work on purely-sparse adapters [SNR21], we show that RoSA adapters can be co-trained in a stable manner, and that they can lead to considerably higher accuracy of the resulting model, at a comparable parameter budget relative to standard adapters that are either low-rank or sparse.

We complement our algorithmic contribution with an efficient system implementation of RoSA in Pytorch, that is aimed at NVIDIA GPUs. The key technical challenge is in supporting sparse adapters with low memory and computational overhead. This is non-trivial as we must leverage unstructured sparse representations that are notoriously hard to support efficiently, especially on GPUs [GZYE20].

In summary, we present promising evidence that the accuracy gap between adaptation methods and full fine-tuning of LLMs can be significantly reduced or even eliminated, without sacrificing practical accessibility. Therefore, RoSA can be an additional technique in the toolbox of machine learning practitioners, specifically for those working with LLMs in resource-constrained settings.

2 Related Work

Parameter-Efficient Fine-Tuning. Recent LLMs such as LLaMA [TLI⁺23], LLaMA2 [TMS⁺23], OPT [ZRG⁺22], and MPT [Tea23] have demonstrated exceptional performance across various natural language processing tasks. However, their substantial size, reaching tens or hundreds of billions of parameters, presents challenges during training due to high memory and computation demands. The common practice is to fine-tune these models on smaller downstream tasks rather than training them from scratch [MLZH21, WBZ⁺21, OWJ⁺22, WMA⁺22, WKM⁺22, LTM⁺22]. While this approach partially addresses the computation demands, memory requirements persist as a concern. Parameter-Efficient Fine-Tuning (PEFT) methods have emerged as a solution to this issue [HSW⁺21, ZCB⁺23, LL21, LJP⁺21, LZD⁺23, LARC21, LTM⁺22, SWR⁺21, HWYBO21, ETK⁺22, LYL⁺23, QLF⁺23, SNR21]. Instead of fine-tuning all parameters, these methods selectively fine-tune a smaller set of parameters, potentially including a subset of the original ones. Notably, LoRA-type methods [HSW⁺21, ZCB⁺23], which train a low-rank perturbation to the original weights, have gained popularity for their efficiency and ease of use [DPHZ23, LHR23]. However, it is known that LoRA often fails to fully recover the accuracy of FFT [ETK⁺22, ZCB⁺23]. FISH Mask [SNR21] updates only a sparse subset of weights in the BERT-base model [DCLT18]. Its reliance on the Fisher Information Matrix (FIM) for generating sparsity masks renders it impractical for LLMs, unless approximations are employed. FISH Mask uses the empirical diagonal estimation of the FIM, but in Section 5 we find it to be not particularly effective in the case of LLMs.

Sparse Training / Fine-Tuning. Inducing and leveraging sparsity in language models has emerged as a popular strategy to address their significant computational and memory demands [HABN⁺21], both for inference [KKF⁺23, KCN⁺22, SA20, FA22a, SWR20, FA23, FA22b, KFA23, GEH19] and training [NPI⁺23, EGM⁺20, PIVA21, HCI⁺21, JHS22]. Sparse training aims to introduce and take advantage of sparsity throughout the training process, providing a faster and less memory-exhaustive training. Another related research direction is sparse fine-tuning, where a network, pre-trained and sparsified on an upstream dataset, undergoes fine-tuning on a downstream task while keeping the sparsity mask fixed [NPI⁺23, KCN⁺22, KKF⁺23]. Despite both sparse fine-tuning and sparse adaptation optimizing over a fixed subset of parameters, they exhibit a crucial difference: in sparse fine-tuning, the weights not involved are pruned (fixed at zero), whereas in sparse adaptation, they are merely frozen, possibly at non-zero values. This distinction allows us to achieve extremely high sparsity levels in sparse adaptation masks (over 99%, as discussed in Section 5), whereas sparse training / fine-tuning typically struggle to exceed 90-95% without significant accuracy loss.

Robust Principal Component Analysis (RPCA). RPCA is a well-explored domain, focusing on techniques that can effectively handle data corrupted by outliers or gross errors. Classical Principal Component Analysis (PCA) assumes that the data is clean, making it prone to breakdown in the presence of noise or outliers. To address this limitation, RPCA methods have been developed to extract robust principal components even in the presence of significant outliers [WGR⁺09, CLMW11, DLTB03, Hub04, KK05, GK72, FB81]. Specifically, given noisy measurements expressed as $A = L + S$, where L is low-rank and S is sparsely supported with elements of arbitrary large magnitude, the goal is to recover L and S . While early approaches failed to achieve this in polynomial running time [DLTB03, Hub04, KK05, GK72, FB81], recent papers show that it is possible to relax the optimization problem by substituting the low-rank constraint on L with a constraint on its nuclear norm, and the sparsity constraint of S with an ℓ_1 constraint. The resulting optimization problem is convex, and has been proved to recover the original matrices under broad assumptions [WGR⁺09, CLMW11]. By contrast to this line of work, we perform Robust PCA-type optimization over a series of adapter matrices that are being learned jointly in an LLM. As such, existing theoretical mechanisms do not apply. Extending them would be an interesting question for future work.

System Support for Sparsity. With advancements in sparsity algorithms, efforts have been directed towards enhancing system support for sparsity. PyTorch [PGM⁺19] has recently incorporated partial sparsity support, and STen [IDH22] has introduced an interface facilitating the integration of sparsity-related algorithms into the PyTorch framework. An important motivation behind sparse models is to exploit sparsity for faster and more efficient inference. PyTorch [PGM⁺19] supports sparse operations for linear models on both GPU and CPU, while DeepSparse [Dee21] and sputnik [GZYE20] offer more specialized support for unstructured sparse operations on CPU and GPU, respectively. Additionally, novel sparse formats have been introduced with effective implementations to maximize sparsity utilization within those formats. Notably, OpenAI has introduced efficient GPU kernels tailored for block-sparse weights [GRK17], and NVIDIA has provided Tensor Cores enabling fast computations for N:M sparsity patterns, where only N elements are non-zero in every block of M elements [MLP⁺21]. Leveraging sparsity during backpropagation to expedite training has only recently gained attention in the literature. [HCI⁺21] introduces transposable N:M masks for accelerating both backpropagation and inference, and [NPI⁺23] provides algorithms and implementations for efficient unstructured sparse backpropagation on CPU. Finally, [LOH22] offers an efficient implementation for sparse low-precision operations on Tensor Cores, using a custom block-wise semi-structured sparsity format.

3 Adaptation of Large Language Models

3.1 Notation

Assuming \mathcal{N} represents a pre-trained Large Language Model (LLM), let $\mathcal{W} = \{\mathbf{W}_1, \mathbf{W}_2, \dots, \mathbf{W}_k\}$ denote a sequence containing all fully connected weights of \mathcal{N} , including embedding and sub-attention layers, with $\mathbf{W}_i \in \mathbb{R}^{m_i \times n_i}$ for all $1 \leq i \leq k$. Let vector $\bar{w} \in \mathbb{R}^d$ indicate the rest of \mathcal{N} 's parameters (biases, normalization parameters, etc.) concatenated into a single vector. Given a dataset \mathcal{D} and a loss function $\mathcal{L}(\mathcal{D}; \mathcal{W}, \bar{w})$, full fine-tuning (FFT) of \mathcal{N} on \mathcal{D} can be formulated as solving the following optimization problem:

$$\min_{\mathcal{W}, \bar{w}} \mathcal{L}(\mathcal{D}; \mathcal{W}, \bar{w}) \quad (1)$$

Given that LLMs typically contain billions of parameters, performing FFT can be slow and computationally expensive. This often renders it challenging or even impossible to execute on standard GPUs. A solution to this involves the application of adapters, which we will now formulate. Let $\Delta = \{\Delta_1, \Delta_2, \dots, \Delta_k\}$ include perturbations to the original fully connected weights, and define $\mathcal{W} + \Delta$ as their element-wise sum, i.e., $\mathcal{W} + \Delta = \{\mathbf{W}_1 + \Delta_1, \mathbf{W}_2 + \Delta_2, \dots, \mathbf{W}_k + \Delta_k\}$. Also, let vector $\bar{\delta}$ denote a perturbation to \bar{w} . The *adapted* parameters are then found by solving the following optimization problem:

$$\min_{\Delta, \bar{\delta}} \mathcal{L}(\mathcal{D}; \mathcal{W} + \Delta, \bar{w} + \bar{\delta}), \quad \text{s.t. } \mathcal{C}(\Delta, \bar{\delta}) \quad (2)$$

where $\mathcal{C}(\Delta, \bar{\delta})$ is a set of constraints on the perturbations, aiming to reduce the memory requirements and computational complexity of the optimization problem. Note that an adaptation with no constraints is equivalent to an FFT.

In this context, our exclusive focus is on adaptations where $\bar{\delta} = \mathbf{0}$, as it aligns with standard practice. Nevertheless, given that \bar{w} typically contains significantly fewer parameters than \mathcal{W} , there is room for fine-tuning \bar{w} as well. Also, we are specifically focusing on cases where all fully connected weights undergo adaptation, but our arguments extend trivially to the case where only a subset of these weights are being adapted.

3.2 LoRA: Low-Rank Adaptation

Motivated by the observation that the difference between the original and FFT parameters is approximately low-rank, the well-known Low-Rank Adaptation (LoRA) [HSW⁺21] constrains the perturbations in Δ to exhibit a low rank, specifically the optimization objective will be the following:

$$\min_{\Delta} \mathcal{L}(\mathcal{D}; \mathcal{W} + \Delta, \bar{w}), \quad \text{s.t. } \forall 1 \leq i \leq k : \text{rank}(\Delta_i) \leq r \quad (3)$$

with r being a fixed small number. This approach reduces the number of trainable weights for layer i from $m_i n_i$ to $r(m_i + n_i)$, resulting in accelerated and more memory-efficient fine-tuning.

3.3 SpA: Sparse Adaptation

A Sparse Adaptation (SpA), like [SNR21], imposes high sparsity constraints on perturbations, i.e., the optimization objective will be:

$$\min_{\Delta} \mathcal{L}(\mathcal{D}; \mathcal{W} + \Delta, \bar{w}), \quad \text{s.t. } \forall 1 \leq i \leq k : \|\Delta_i\|_0 \leq d m_i n_i \quad (4)$$

where $d < 1$ represents the perturbation density and $\|\cdot\|_0$ denotes the ℓ_0 norm. Similar to [SNR21], we only consider the case where each perturbation has a fixed support throughout training. This way, SpA reduces the number of trainable parameters by a factor of d . However, it encounters two primary challenges: **1.** The support of each optimal Δ_i (sparsity mask) needs to be efficiently found before initiating fine-tuning. To the best of our knowledge, FISH Mask [SNR21] is the only method that performs SpA, relying on Fisher information to generate the masks, which proves impractical for LLMs unless significant approximations are employed (such as empirical diagonal approximation used in FISH Mask). While we find this approximation to not be effective enough for sparse adaptation (SpA) of LLMs in Section 5, our results show that it suffices for robust adaptation (RoSA), which is introduced in the next subsection. This approach is also justified by its ability to maximize Gradient Flow (GF) early in training, enhancing training

Algorithm 1 Mask Generation

Require: $\mathcal{W}, \bar{w} \leftarrow$ the fully connected weights and the rest of the LLM parameters, respectively
Require: $\mathcal{D}_M \leftarrow$ the mask generation dataset, typically a small subset of the actual dataset
Require: $\mathcal{L}(\cdot) \leftarrow$ the loss function
Require: $d \leftarrow$ mask density

```

 $\mathcal{G} \leftarrow \{0, 0, \dots, 0\}$  [initialize weight gradients with zero]
for each  $s \in \mathcal{D}_M$  do [iterate through samples of  $\mathcal{D}_M$ ]
   $\mathcal{G}^s, \bar{g}^s \leftarrow \nabla \mathcal{L}(s; \mathcal{W}, \bar{w})$  [calculate the gradients for this sample]
   $\mathcal{G} \leftarrow \mathcal{G} + (\mathcal{G}^s)^2$  [accumulate the gradient squares (empirical diagonal fisher)]
end for
for each  $G_i \in \mathcal{G}$  do [iterate through the accumulated gradients of different weights]
   $p_i \leftarrow \text{numel}(G_i)$  [store the number of elements in  $G_i$ ]
   $\mathcal{M}_i \leftarrow \text{TopK-Mask}(G_i, dp_i)$  [choose positions of top-k elements of the accumulated gradient]
end for
return  $\mathcal{M} = \{\mathcal{M}_1, \mathcal{M}_2, \dots, \mathcal{M}_k\}$ 

```

Algorithm 2 Robust Adaptation (RoSA)

Require: $\mathcal{W}, \bar{w} \leftarrow$ the fully connected weights and the rest of the LLM parameters, respectively
Require: $\mathcal{D} \leftarrow$ the downstream dataset
Require: $\mathcal{L}(\cdot) \leftarrow$ the loss function
Require: $r \leftarrow$ LoRA rank
Require: $d \leftarrow$ SpA density
Require: $m \leftarrow$ number of samples to use for mask generation

```

 $\mathcal{D}_M \leftarrow \text{random-subset}(\mathcal{D}, m)$  [take  $m$  random samples of the dataset for mask generation]
 $\mathcal{M} \leftarrow \text{generate-masks}(\mathcal{W}, \bar{w}, \mathcal{D}_M, \mathcal{L}, d)$  [run Algorithm 1 to generate the masks]
 $k \leftarrow \text{length}(\mathcal{W})$  [the number of fully connected weights]
for all  $i \in \{1, 2, \dots, k\}$  do
   $m_i, n_i \leftarrow \text{shape}(\mathcal{W}_i)$  [get the dimensions of  $\mathcal{W}_i$ ]
   $\Delta_i^L \leftarrow \text{initialize-lora-params}(m_i, n_i, r)$  [initialize LoRA params, similar to [HSW+21]]
   $\Delta_i^S \leftarrow \text{initialize-spa-params}(\mathcal{M}_i)$  [initialize SpA params with zero]
end for
 $\Delta^L \leftarrow \{\Delta_1^L, \Delta_2^L, \dots, \Delta_k^L\}$ 
 $\Delta^S \leftarrow \{\Delta_1^S, \Delta_2^S, \dots, \Delta_k^S\}$ 
 $\Delta_*^L, \Delta_*^S \leftarrow \arg \min_{\Delta^L, \Delta^S} \mathcal{L}(\mathcal{D}; \mathcal{W} + \Delta^L + \Delta^S, \bar{w})$  [train the adapters]
return  $\Delta_*^L, \Delta_*^S$ 

```

dynamics [EGM⁺20, EIKD22]. Additionally, [SNR21] shows that this method and the first-order method of averaging gradients over several batches yield similar results on small language models. We make a similar observation for LLMs, as demonstrated in the ablation studies in Section 5. Hence, we adopt the empirical diagonal Fisher estimation for our main experiments, which is equivalent to averaging gradient squares over batches, as described in Algorithm 1. 2. Achieving actual improvements in terms of memory and performance requires the utilization of unstructured sparsity, which is non-trivial especially on GPUs. We offer efficient PyTorch implementations for this, discussed further in Section 4.

3.4 RoSA: Robust Adaptation

Now we will describe our main adaptation method.

Motivation. Approaches akin to LoRA are not without their drawbacks. When faced with more complex downstream tasks, these methods often fail to achieve an accuracy level comparable to full fine-tuning. This limitation arises because such techniques tend to normalize and consequently filter out critical information during the fine-tuning phase. This filtering issue becomes particularly evident when conducting Singular Value Decomposition (SVD) on the Δ^* updates (defined as $\Delta^* = \mathcal{W}^{fft} - \mathcal{W}^{base}$) of LLM layers (as detailed in the Appendix B). These analyses reveal that while Δ^* is rank-deficient (see Figure 3), it is not strictly low-rank. This distinction is characterized by the presence of a substantial fraction of singular values with relatively small but non-zero magnitudes.

The Robust Principal Component Analysis (RPCA) method offers a promising alternative. RPCA effectively decomposes a matrix into two components: a low-rank matrix and a sparse matrix. This decomposition offers a more nuanced approximation of the fine-tuning updates compared to solely low-rank methods. Nonetheless, the RPCA algorithm,

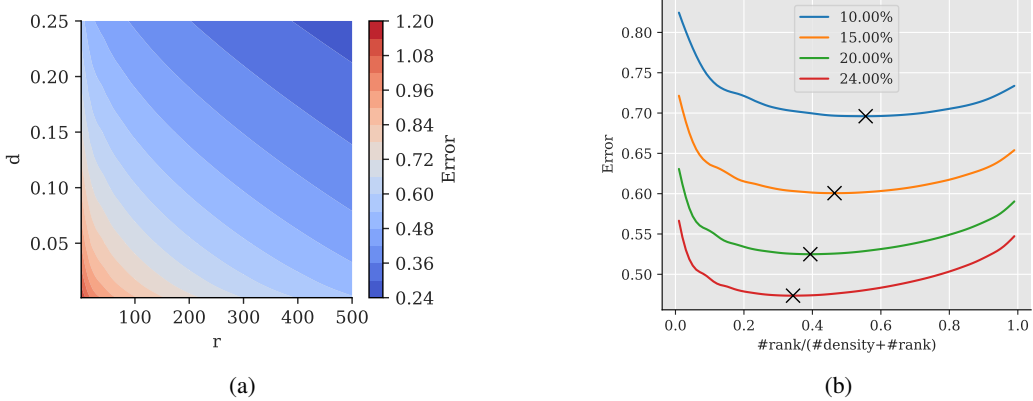


Figure 2: In Figures 2a and 2b, we demonstrate the application of *one-shot RPCA* to the FFT update ($\mathcal{W}_{gsm8k} - \mathcal{W}_{base}$) for a randomly chosen layer (1:20, `v_proj`) of LLaMA2-7B. We varied the low-rank module’s rank and the sparse module’s density to assess the approximation’s effectiveness. The Frobenius norm of the resulting error matrix is plotted in Figure 2a. Figure 2b, which depicts slices of Figure 2a with similar parameter count, showcases the trade-off between sparsity and low-rank under different parameter budgets, highlighting that a combined approach of low-rank and sparse methods yields superior performance in approximating the FFT update within a specified parameter budget. The notation `#rank` and `#density` represent the number of parameters induced by low-rank and sparse approximations, respectively. i.e., the rightmost part of Figure 2b represents the case where all the budget is spent on the low-rank module and the sparse module is ignored.

with its multiple iterations of SVD, presents practical challenges when applied to high-dimensional matrices, such as those in LLaMA2 [TMS⁺23]. To circumvent this issue, we employ a simplified version of RPCA, effectively a single-iteration variant which we call *one-shot RPCA*. This adaptation still captures the essence of the original RPCA while being more feasible for large-scale matrices.

In Figure 2a, we have analyzed a randomly selected module from LLaMA2-7B, computed its Δ^* when fine-tuned on the GSM8k dataset, and then applied a *one-shot RPCA* (i.e., single iteration) with varying ranks and densities for the low-rank and sparse components. The results in Figure 2b clearly demonstrate that, given a parameter budget to approximate Δ^* , employing a combination of low-rank and sparse approximations yields a more accurate representation than using either approach in isolation.

Lastly, it is crucial to note that our usage of RPCA is primarily for the analysis of fine-tuning updates. This analysis is independent of our proposed method, RoSA, which utilizes a combination of low-rank and sparse fine-tuning. The link between RPCA and RoSA lies in the former’s introduction of the low-rank and sparse decomposition, a concept we leverage in RoSA to enhance the efficiency and accuracy of fine-tuning LLMs.

Formulation. Equipped with this motivation, we formulate the optimization objective of Robust Adaptation (RoSA) as follows:

$$\min_{\Delta^L, \Delta^S} \mathcal{L}(\mathcal{D}; \mathcal{W} + \Delta^L + \Delta^S, \bar{w}), \quad s.t. \quad \forall 1 \leq i \leq k : \begin{cases} \text{rank}(\Delta_i^L) \leq r \\ \|\Delta_i^S\|_0 \leq dm_i n_i \end{cases} \quad (5)$$

where Δ^L and Δ^S represent the low-rank and sparse adapters, respectively. In practice, we generate the sparsity masks using Algorithm 1, and then optimize the low-rank and sparse adapters jointly. Refer to Algorithm 2 and Figure 1b for a detailed description of RoSA.

4 System Implementation

We implement all adaptation methods into the `11m-foundry` codebase [ML23]. For LoRA, we utilized the official Microsoft implementation [HSW⁺21]. Our kernels for performing sparse operations on GPU are based on the `sputnik` library [GZYE20]. Next, we will elaborate on the implementation of RoSA.

Low-Rank Format. Similar to [HSW⁺21], we store an $m \times n$ low-rank adapter with rank r as the multiplication of two matrices $\mathbf{B}\mathbf{A}$, where \mathbf{B} and \mathbf{A} are $m \times r$ and $r \times n$, respectively.

Sparse Format. Sparse adapters are stored in Compressed Sparse Row (CSR) format, which utilizes three lists to represent an $m \times n$ sparse matrix with nnz non-zero values: a `values` list with size nnz , storing the non-zero values; a `row-offsets` list with size $m + 1$, indicating the position of the first non-zero element in each row within the `values` list; and a `column-indices` list with size nnz , containing the column index of each corresponding element in the `values` list. Additionally, in line with [GZYE20], an extra `row-indices` list with size m is included, sorting rows based on their non-zero element count. This `row-indices` list is employed by `sputnik` [GZYE20] for load-balancing purposes.

Forward Pass. Consider a single fully connected layer with an adapted weight matrix $\mathbf{W} + \Delta^L + \Delta^S$ of size $m \times n$. For simplicity, assume there is no bias vector. Given a batch of inputs \mathbf{X} of size $b \times m$, the output of this layer is expressed as:

$$\mathbf{O} = \mathbf{X}(\mathbf{W} + \Delta^L + \Delta^S) = \mathbf{X}\mathbf{W} + (\mathbf{X}\mathbf{B}^L)\mathbf{A}^L + \mathbf{X}\Delta^S \quad (6)$$

While the first two terms can be calculated using standard matrix multiplication, the term $\mathbf{X}\Delta^S$ requires Sparse Matrix-Matrix Multiplication (SpMM), which is efficiently supported by `sputnik` [GZYE20]. It is worth noting that the multiplication in the second term is decomposed into two multiplications with low-rank, making it extremely fast.

Backward Pass. Given the gradients of the output $\frac{\partial \mathcal{L}}{\partial \mathbf{O}}$, the backward pass through this layer involves calculating the gradients of the parameters and the inputs, given by the following equations.

$$\frac{\partial \mathcal{L}}{\partial \mathbf{X}} = \frac{\partial \mathcal{L}}{\partial \mathbf{O}}(\mathbf{W} + \Delta^L + \Delta^S)^T = \frac{\partial \mathcal{L}}{\partial \mathbf{O}}\mathbf{W}^T + \left(\frac{\partial \mathcal{L}}{\partial \mathbf{O}}(\mathbf{A}^L)^T\right)(\mathbf{B}^L)^T + \frac{\partial \mathcal{L}}{\partial \mathbf{O}}(\Delta^S)^T \quad (7)$$

$$\frac{\partial \mathcal{L}}{\partial \mathbf{B}^L} = \frac{\partial \mathcal{L}}{\partial (\mathbf{B}^L \mathbf{A}^L)}(\mathbf{A}^L)^T = \mathbf{X}^T \left(\frac{\partial \mathcal{L}}{\partial \mathbf{O}}(\mathbf{A}^L)^T\right) \quad (8)$$

$$\frac{\partial \mathcal{L}}{\partial \mathbf{A}^L} = (\mathbf{B}^L)^T \frac{\partial \mathcal{L}}{\partial (\mathbf{B}^L \mathbf{A}^L)} = \left((\mathbf{B}^L)^T \mathbf{X}^T\right) \frac{\partial \mathcal{L}}{\partial \mathbf{O}} \quad (9)$$

$$\frac{\partial \mathcal{L}}{\partial \Delta^S} = \mathbf{X}^T \frac{\partial \mathcal{L}}{\partial \mathbf{O}} \quad (10)$$

Except for the transposition of Δ^S , which we will discuss in the next paragraph, equations 7, 8, and 9 can be computed efficiently using similar tricks as equation 6. However, equation 10 involves multiplying two dense matrices, and only specific elements of the output are needed. Similar to [NPI⁺23], we employ a Sampled Dense-Dense Matrix Multiplication (SDDMM) to perform this operation, which is again supported by the `sputnik` [GZYE20] library.

Transposition. As evident from the above equations, transposing the sparse matrix Δ^S is necessary at every backward pass. Doing this naively is slow and impact performance significantly. Consequently, we adopted a trick to expedite transposition, even though it slightly increases memory usage. Notice that since the support of Δ^S is fixed, the support of its transposition is also fixed. Therefore, we transpose it once and reuse the transposed index lists `row-offsets`, `column-indices`, and `row-indices`. Regarding the transposed `values` list, we observe that it is always a fixed permutation of the original `values` list. Hence, we store this permutation, resulting in the cost of every transposition being merely a permutation of the `values` list.

Mask Generation. As explained in Algorithm 1, creating the masks involves keeping track of full gradients, which can be challenging in terms of memory. Yet, we adopt a straightforward solution by transferring the gradients of each weight matrix to CPU as soon as they are computed. This ensures that at most one weight matrix’s gradient is stored on GPU at any given time.

5 Experiments

In this section, we provide experimental support for the effectiveness of RoSA. The following subsection outlines the experiment settings, including details on the network and datasets. To ensure a fair comparison, we conducted thorough and careful tuning for each adaptation method, details of which are described next. We then present the results, along

with ablation studies, showcasing the improvements achieved by RoSA. Finally, we assess RoSA’s resource utilization in terms of memory and time, highlighting that it requires only slightly more resources than LoRA and SpA while offering significantly improved accuracy.

5.1 Settings

Model and Datasets. We perform fine-tuning of the LLaMA2-7B model [TMS⁺23] on three standard datasets: ViGGO [JBW19], GSM8k [CKB⁺21], and SQL generation [ZXS17, YZY⁺18], containing $5.1k$, $7.47k$, and $30k$ training samples and $1.08k$, $1.32k$, and $1k$ test samples, respectively. Refer to Appendix A for examples of the GSM8k dataset. In the case of SQL, we follow the dataset formation strategy described in [NHA23]. On GSM8k, we only consider the accuracy of the final answer. Notably, these datasets are chosen such that they are highly specialized, and therefore require fine-tuning for good performance: for example, on GSM8k, the original pre-trained model has zero one-shot accuracy, and the multi-shot accuracy is also very poor (around 6%).

Hyperparameters. In all experiments, we use a standard batch size of 32 (micro batch size 1 + gradient accumulation) and a maximum context length of 512, which matches the dataset sample structure. We employ the AdamW optimizer [LH17] with parameters $\beta_1 = 0.9$, $\beta_2 = 0.999$, $\epsilon = 10^{-8}$, and a linear learning rate scheduler with 20 batches warmup. Notably, all floating-point values are stored in the `bfloat16` format [DCM⁺12]: this is very popular due to low memory usage and good accuracy. Our main experiments run for a single epoch, but we demonstrate in ablation studies that extended training can further improve adaptation results. Following [HSW⁺21], we use $\alpha = 16$ and a dropout of 0.05 for the low-rank adapter, while experimenting with various r values ranging from 4 to 64. Additionally, we set the size of the mask generation dataset to 1 batches in the main experiment, but we also consider larger number of batches in the ablation studies.

The sparse adapter’s density ranges from 0.15% to 2.4%. While it is possible to adapt only a subset of the linear layers in the model, we specifically consider the case where every embedding and fully connected layer undergo adaptation. This choice is motivated by the significantly lower memory usage of adaptation parameters compared to storing the original parameters (see Table 1). The best learning rates for FFT are 9×10^{-6} , 1×10^{-5} , and 3×10^{-5} on SQL, ViGGO, and GSM8k, respectively. The best-performing learning rates are selected in the range $[10^{-4}, 10^{-3}]$ and $[10^{-4}, 8 \times 10^{-4}]$ for LoRA and SpA parameters, respectively. In RoSA experiments, we find it beneficial to initially fine-tune solely with LoRA for 64 batches, generate and fix the sparse masks, and restart training with both LoRA and sparse adaptation (SpA) activated. Finally, nearly all experiments comfortably run on a single NVIDIA GeForce RTX 3090 GPU with a memory size of 24.3 GB, except for FFT and a few of the largest-budget adaptation experiments (refer to Table 1).

5.2 Results

Main Experiment. In Table 1, we summarize our main experiments, which examine the accuracy of various fine-tuning approaches, at various budgets, across all the tasks considered. We consider three parameter budgets: 40 millions, 80 millions, and 160 millions. For each budget, we explore five different ways of distributing parameters between LoRA and SpA, ranging from pure LoRA/SpA to intermediate sparse + low-rank budgets. The main experiments are conducted for a standard single pass over the dataset (epoch). However, for the smaller ViGGO and GSM8k datasets, we observe that extended training improves adaptation results. Hence, we also present the best results, for each method, from 2 and 3 epochs on these two datasets, under the ‘Extended’ label. (We did not run extended training on SQL due to its much larger size.)

Single-Pass Runs. The results in Table 1 show that, across all tasks and budgets, RoSA outperforms both LoRA and SpA. In the single-epoch regime, RoSA surprisingly even surpasses FFT significantly on the ViGGO and SQL datasets, while nearly matching FFT performance on GSM8k (31.3% vs 31.8%). This shows that this approach can be particularly effective in the context of short, single-pass training, across tasks and parameter budgets.

Extended Experiments. The above conclusion persists in the extended experiments, where we find that RoSA can in fact match FFT on both GSM8k and ViGGO. The fact that the best results for extended training are obtained on the small and medium-sized parameter budgets suggest that the computational budget should be balanced against the active parameters for the run: the largest budget yields highest performance only on the large SQL dataset.

Overall, these results clearly highlight the effectiveness of RoSA; specifically, we find it remarkable that we are able to fully recover FFT accuracy while using parameter budgets that are 40-100x smaller. Finally, please also note that the memory overheads of maintaining sparse and low-rank components are low: up to the 80M parameter budget, all our experiments fit inside a single 24GB GPU, and the memory overhead of RoSA relative to LoRA is within 2GB for this model/task setup.

	#Parameters	Memory	GSM8k		ViGGO		SQL
			1 Epoch	Extended	1 Epoch	Extended	1 Epoch
FFT	6.7 B	> 60 GB	31.8	37.5	94.0	96.8	89.4
LoRA $r = 16$	41.1 M	20.8 GB	24.3	32.1	78.7	93.1	87.7
RoSA $r = 12, d = 0.15\%$	41.0 M	22.2 GB	29.3	37.5	93.8	96.5	88.3
RoSA $r = 8, d = 0.3\%$	40.8 M	22.3 GB	29.6	37.1	94.8	96.5	87.9
RoSA $r = 4, d = 0.45\%$	40.6 M	22.4 GB	28.4	32.9	90.5	96.1	87.5
SpA $d = 0.6\%$	40.4 M	20.9 GB	26.3	31.4	78.0	94.1	87.3
LoRA $r = 32$	82.3 M	21.1 GB	27.9	33.5	72.4	95.8	88.1
RoSA $r = 24, d = 0.3\%$	81.9 M	22.6 GB	29.9	35.4	93.4	96.4	88.6
RoSA $r = 16, d = 0.6\%$	81.6 M	22.8 GB	31.1	36.9	95.5	96.8	88.3
RoSA $r = 8, d = 0.9\%$	81.2 M	23.1 GB	31.3	37.1	93.4	96.2	87.9
SpA $d = 1.2\%$	80.9 M	21.6 GB	27.3	31.6	89.3	94.5	89.4
LoRA $r = 64$	164.5 M	21.8 GB	25.1	34.4	85.3	95.0	87.7
RoSA $r = 48, d = 0.6\%$	163.8 M	23.6 GB	30.0	34.3	92.2	96.6	88.5
RoSA $r = 32, d = 1.2\%$	163.1 M	24.0 GB	30.2	35.0	95.7	96.6	88.1
RoSA $r = 16, d = 1.8\%$	162.4 M	24.5 GB	31.1	35.9	94.9	96.2	89.8
SpA $d = 2.4\%$	161.7 M	23.4 GB	29.7	35.3	92.0	95.9	87.9

Table 1: Comparison of fine-tuning LLaMA2-7B using FFT, LoRA, SpA, and RoSA in terms of memory usage and accuracy on three datasets. While fine-tuning LLMs for a single epoch is standard, we include results of extended training (best of 2 and 3 epochs) in the case of smaller datasets (GSM8k and ViGGO) to study the improvements achieved by extended training.

Mask Generation. We investigate the impact of different mask generation methods on RoSA results for the GSM8k dataset in Table 2. The considered methods are: (1) second-order empirical diagonal Fisher estimation, and (2) first-order gradient averaging. For each method, we explore calculating the masks using both 1 and 8 batches of data. Consistent with findings in [SNR21], we observe that these two methods do not show a significant difference in the final training accuracy.

Moreover, we note a positive impact on the accuracy by increasing the size of \mathcal{D}_M (the mask generation dataset, see Algorithms 1). Although Table 1 revealed that RoSA fell short of matching FFT accuracy only in the single-epoch GSM8k case, increasing the size of \mathcal{D}_M to 8 batches (256 samples) enables RoSA to effectively outperform FFT in that scenario as well. This emphasizes the importance of selecting an accurate mask. The inaccuracy of diagonal approximation of the empirical Fisher matrix highlights the need for more precise methods to efficiently generate an accurate mask for RoSA. Although more accurate methods, such as block-diagonal approximation [SA20], do exist, they typically demand a higher amount of memory and longer running times, both of which are constrained in our setting. Consequently, we leave the exploration of these methods to future work.

6 Discussion

In this paper, we took a step forward in to address the problem of efficient fine-tuning of Large Language Models (LLMs). Motivated by the observation that the sum of gradient updates performed by full fine-tuning (FFT) is well-approximated by the sum of low-rank and sparse matrices, we proposed a method called Robust Adaptation (RoSA), which is inspired by the Robust PCA approach. We show that RoSA significantly outperforms both low-rank adaptation (LoRA) [HSW⁺21] and sparse adaptation (SpA) [SNR21] at the same parameter budgets. Additionally, we came across the surprising observation that the best performing RoSA can match or even outperform FFT in many settings. Moreover, we highlight the need for better criteria to generate the mask required by sparse adaptation, which we leave

	# Parameters	Diag-Fisher		Avg-Grad	
		1 Batch	8 Batches	1 Batch	8 Batches
RoSA $r = 12, d = 0.15\%$	41.0 M	29.3	29.5	29.3	29.5
RoSA $r = 8, d = 0.3\%$	40.8 M	29.6	29.7	29.6	29.2
RoSA $r = 4, d = 0.45\%$	40.6 M	28.4	29.2	28.8	29.2
SpA $d = 0.6\%$	40.4 M	26.3	25.7	23.8	25.7
RoSA $r = 24, d = 0.3\%$	81.9 M	29.9	29.9	29.9	29.9
RoSA $r = 16, d = 0.6\%$	81.6 M	31.1	31.1	30.4	31.1
RoSA $r = 8, d = 0.9\%$	81.2 M	31.3	30.5	31.3	30.5
SpA $d = 1.2\%$	80.9 M	27.3	28.1	29.2	28.1
RoSA $r = 48, d = 0.6\%$	163.8 M	30.0	31.8	30.0	31.8
RoSA $r = 32, d = 1.2\%$	163.1 M	30.2	29.6	30.2	29.6
RoSA $r = 16, d = 1.8\%$	162.4 M	31.1	32.1	31.0	32.1
SpA $d = 2.4\%$	161.7 M	29.7	27.6	29.2	27.6

Table 2: A comparison between employing empirical diagonal Fisher approximation (Diag-Fisher) and gradient averaging (Avg-Grad) for mask generation. The experiments are single-epoch and performed on the GSM8k dataset. For each approach, we consider using 1 and 8 batches of data (32 and 256 samples as batch size is 32) for generating the masks.

for future work. To complement our contributions, we offer an efficient PyTorch implementation of our method, aiming to make RoSA an accessible tool for researchers in the field.

Acknowledgments

The authors would like to thank Eldar Kurtic for experimental support and useful suggestions throughout the project.

References

- [ABC²¹] Amanda Askell, Yuntao Bai, Anna Chen, Dawn Drain, Deep Ganguli, Tom Henighan, Andy Jones, Nicholas Joseph, Ben Mann, Nova DasSarma, et al. A general language assistant as a laboratory for alignment. *arXiv preprint arXiv:2112.00861*, 2021.
- [BJN²²] Yuntao Bai, Andy Jones, Kamal Ndousse, Amanda Askell, Anna Chen, Nova DasSarma, Dawn Drain, Stanislav Fort, Deep Ganguli, Tom Henighan, et al. Training a helpful and harmless assistant with reinforcement learning from human feedback. *arXiv preprint arXiv:2204.05862*, 2022.
- [CKB²¹] Karl Cobbe, Vineet Kosaraju, Mohammad Bavarian, Mark Chen, Heewoo Jun, Lukasz Kaiser, Matthias Plappert, Jerry Tworek, Jacob Hilton, Reiichiro Nakano, Christopher Hesse, and John Schulman. Training verifiers to solve math word problems. *arXiv preprint arXiv:2110.14168*, 2021.
- [CLMW11] Emmanuel J Candès, Xiaodong Li, Yi Ma, and John Wright. Robust principal component analysis? *Journal of the ACM (JACM)*, 58(3):1–37, 2011.
- [DCLT18] Jacob Devlin, Ming-Wei Chang, Kenton Lee, and Kristina Toutanova. Bert: Pre-training of deep bidirectional transformers for language understanding. *arXiv preprint arXiv:1810.04805*, 2018.
- [DCM¹²] Jeffrey Dean, Greg Corrado, Rajat Monga, Kai Chen, Matthieu Devin, Mark Mao, Marc’ aurelio Ranzato, Andrew Senior, Paul Tucker, Ke Yang, et al. Large scale distributed deep networks. *Advances in neural information processing systems*, 25, 2012.
- [Dee21] DeepSparse. NeuralMagic DeepSparse Inference Engine, 2021.
- [DLBZ22] Tim Dettmers, Mike Lewis, Younes Belkada, and Luke Zettlemoyer. LLM.int8(): 8-bit matrix multiplication for transformers at scale. *Advances in Neural Information Processing Systems 35: Annual Conference on Neural Information Processing Systems 2022, NeurIPS 2022*, 2022.

- [DLTB03] Fernando De La Torre and Michael J Black. A framework for robust subspace learning. *International Journal of Computer Vision*, 54:117–142, 2003.
- [DPHZ23] Tim Dettmers, Artidoro Pagnoni, Ari Holtzman, and Luke Zettlemoyer. Qlora: Efficient finetuning of quantized llms. *arXiv preprint arXiv:2305.14314*, 2023.
- [DSE⁺23] Tim Dettmers, Ruslan Svirschevski, Vage Egiazarian, Denis Kuznedelev, Elias Frantar, Saleh Ashkboos, Alexander Borzunov, Torsten Hoefer, and Dan Alistarh. Spqr: A sparse-quantized representation for near-lossless llm weight compression. *arXiv preprint arXiv:2306.03078*, 2023.
- [EGM⁺20] Utku Evci, Trevor Gale, Jacob Menick, Pablo Samuel Castro, and Erich Elsen. Rigging the lottery: Making all tickets winners. In *International Conference on Machine Learning*, pages 2943–2952. PMLR, 2020.
- [EIKD22] Utku Evci, Yani Ioannou, Cem Keskin, and Yann Dauphin. Gradient flow in sparse neural networks and how lottery tickets win. In *Proceedings of the AAAI conference on artificial intelligence*, volume 36, pages 6577–6586, 2022.
- [ETK⁺22] Ali Edalati, Marzieh Tahaei, Ivan Kobyzev, Vahid Partovi Nia, James J Clark, and Mehdi Rezagholizadeh. Krona: Parameter efficient tuning with kronecker adapter. *arXiv preprint arXiv:2212.10650*, 2022.
- [FA22a] Elias Frantar and Dan Alistarh. Optimal brain compression: A framework for accurate post-training quantization and pruning. *Advances in Neural Information Processing Systems*, 35:4475–4488, 2022.
- [FA22b] Elias Frantar and Dan Alistarh. Spdy: Accurate pruning with speedup guarantees. In *International Conference on Machine Learning*, pages 6726–6743. PMLR, 2022.
- [FA23] Elias Frantar and Dan Alistarh. Sparsegpt: Massive language models can be accurately pruned in one-shot. In *International Conference on Machine Learning*, pages 10323–10337. PMLR, 2023.
- [FB81] Martin A Fischler and Robert C Bolles. Random sample consensus: a paradigm for model fitting with applications to image analysis and automated cartography. *Communications of the ACM*, 24(6):381–395, 1981.
- [GEH19] Trevor Gale, Erich Elsen, and Sara Hooker. The state of sparsity in deep neural networks. *arXiv preprint arXiv:1902.09574*, 2019.
- [GK72] Ramanathan Gnanadesikan and John R Kettenring. Robust estimates, residuals, and outlier detection with multiresponse data. *Biometrics*, pages 81–124, 1972.
- [GRK17] Scott Gray, Alec Radford, and Diederik P Kingma. Gpu kernels for block-sparse weights. *arXiv preprint arXiv:1711.09224*, 3(2):2, 2017.
- [GZYE20] Trevor Gale, Matei Zaharia, Cliff Young, and Erich Elsen. Sparse GPU kernels for deep learning. In *Proceedings of the International Conference for High Performance Computing, Networking, Storage and Analysis, SC 2020*, 2020.
- [HABN⁺21] Torsten Hoefer, Dan Alistarh, Tal Ben-Nun, Nikoli Dryden, and Alexandra Peste. Sparsity in deep learning: Pruning and growth for efficient inference and training in neural networks. *The Journal of Machine Learning Research*, 22(1):10882–11005, 2021.
- [HCI⁺21] Itay Hubara, Brian Chmiel, Moshe Island, Ron Banner, Joseph Naor, and Daniel Soudry. Accelerated sparse neural training: A provable and efficient method to find n: m transposable masks. *Advances in neural information processing systems*, 34:21099–21111, 2021.
- [HSW⁺21] Edward J Hu, Yelong Shen, Phillip Wallis, Zeyuan Allen-Zhu, Yuanzhi Li, Shean Wang, Lu Wang, and Weizhu Chen. Lora: Low-rank adaptation of large language models. *arXiv preprint arXiv:2106.09685*, 2021.
- [Hub04] Peter J Huber. *Robust statistics*, volume 523. John Wiley & Sons, 2004.
- [HWYBO21] Nam Hyeon-Woo, Moon Ye-Bin, and Tae-Hyun Oh. Fedpara: Low-rank hadamard product for communication-efficient federated learning. *arXiv preprint arXiv:2108.06098*, 2021.
- [IDH22] Andrei Ivanov, Nikoli Dryden, and Torsten Hoefer. Sten: An interface for efficient sparsity in pytorch. 2022.
- [JBW19] Juraj Juraska, Kevin Bowden, and Marilyn Walker. ViGGO: A video game corpus for data-to-text generation in open-domain conversation. In *Proceedings of the 12th International Conference on Natural Language Generation*, pages 164–172, Tokyo, Japan, October–November 2019. Association for Computational Linguistics.

- [JHS22] Peng Jiang, Lihan Hu, and Shihui Song. Exposing and exploiting fine-grained block structures for fast and accurate sparse training. *Advances in Neural Information Processing Systems*, 35:38345–38357, 2022.
- [KCN⁺22] Eldar Kurtic, Daniel Campos, Tuan Nguyen, Elias Frantar, Mark Kurtz, Benjamin Fineran, Michael Goin, and Dan Alistarh. The optimal bert surgeon: Scalable and accurate second-order pruning for large language models. *arXiv preprint arXiv:2203.07259*, 2022.
- [KFA23] Eldar Kurtic, Elias Frantar, and Dan Alistarh. Ziplm: Hardware-aware structured pruning of language models. *arXiv preprint arXiv:2302.04089*, 2023.
- [KK05] Qifa Ke and Takeo Kanade. Robust l₁/sub 1/norm factorization in the presence of outliers and missing data by alternative convex programming. In *2005 IEEE Computer Society Conference on Computer Vision and Pattern Recognition (CVPR'05)*, volume 1, pages 739–746. IEEE, 2005.
- [KKF⁺23] Eldar Kurtic, Denis Kuznedelev, Elias Frantar, Michael Goin, and Dan Alistarh. Sparse finetuning for inference acceleration of large language models. *arXiv preprint arXiv:2310.06927*, 2023.
- [LARC21] Brian Lester, Rami Al-Rfou, and Noah Constant. The power of scale for parameter-efficient prompt tuning. *arXiv preprint arXiv:2104.08691*, 2021.
- [LH17] Ilya Loshchilov and Frank Hutter. Decoupled weight decay regularization. *arXiv preprint arXiv:1711.05101*, 2017.
- [LHR23] Ariel N Lee, Cole J Hunter, and Nataniel Ruiz. Platypus: Quick, cheap, and powerful refinement of llms. *arXiv preprint arXiv:2308.07317*, 2023.
- [LJF⁺21] Xiao Liu, Kaixuan Ji, Yicheng Fu, Weng Lam Tam, Zhengxiao Du, Zhilin Yang, and Jie Tang. P-tuning v2: Prompt tuning can be comparable to fine-tuning universally across scales and tasks. *arXiv preprint arXiv:2110.07602*, 2021.
- [LL21] Xiang Lisa Li and Percy Liang. Prefix-tuning: Optimizing continuous prompts for generation. *arXiv preprint arXiv:2101.00190*, 2021.
- [LOH22] Shigang Li, Kazuki Osawa, and Torsten Hoefer. Efficient quantized sparse matrix operations on tensor cores. In *SC22: International Conference for High Performance Computing, Networking, Storage and Analysis*, pages 1–15. IEEE, 2022.
- [LTM⁺22] Haokun Liu, Derek Tam, Mohammed Muqeeth, Jay Mohta, Tenghao Huang, Mohit Bansal, and Colin A Raffel. Few-shot parameter-efficient fine-tuning is better and cheaper than in-context learning. *Advances in Neural Information Processing Systems*, 35:1950–1965, 2022.
- [LYL⁺23] Yixiao Li, Yifan Yu, Chen Liang, Pengcheng He, Nikos Karampatziakis, Weizhu Chen, and Tuo Zhao. Loftq: Lora-fine-tuning-aware quantization for large language models. *arXiv preprint arXiv:2310.08659*, 2023.
- [LZD⁺23] Xiao Liu, Yanan Zheng, Zhengxiao Du, Ming Ding, Yujie Qian, Zhilin Yang, and Jie Tang. Gpt understands, too. *AI Open*, 2023.
- [ML23] Mosaic ML. LLM Foundry, 2023.
- [MLP⁺21] Asit Mishra, Jorge Albericio Latorre, Jeff Pool, Darko Stosic, Dusan Stosic, Ganesh Venkatesh, Chong Yu, and Paulius Micikevicius. Accelerating sparse deep neural networks. *arXiv preprint arXiv:2104.08378*, 2021.
- [MLZH21] Sewon Min, Mike Lewis, Luke Zettlemoyer, and Hannaneh Hajishirzi. Metacl: Learning to learn in context. *arXiv preprint arXiv:2110.15943*, 2021.
- [NHA23] Artur Niederfahrenhorst, Kourosh Hakhamaneshi, and Rehaan Ahmad. Fine-Tuning LLMs: LoRA or Full-Parameter?, 2023.
- [NPI⁺23] Mahdi Nikdan, Tommaso Pegolotti, Eugenia Iofinova, Eldar Kurtic, and Dan Alistarh. Sparseprop: Efficient sparse backpropagation for faster training of neural networks at the edge. In *International Conference on Machine Learning*, pages 26215–26227. PMLR, 2023.
- [OWJ⁺22] Long Ouyang, Jeffrey Wu, Xu Jiang, Diogo Almeida, Carroll Wainwright, Pamela Mishkin, Chong Zhang, Sandhini Agarwal, Katarina Slama, Alex Ray, et al. Training language models to follow instructions with human feedback. *Advances in Neural Information Processing Systems*, 35:27730–27744, 2022.
- [PGM⁺19] Adam Paszke, Sam Gross, Francisco Massa, Adam Lerer, James Bradbury, Gregory Chanan, Trevor Killeen, Zeming Lin, Natalia Gimelshein, Luca Antiga, et al. Pytorch: An imperative style, high-performance deep learning library. In *Advances in Neural Information Processing Systems*, 2019.

- [PIVA21] Alexandra Peste, Eugenia Iofinova, Adrian Vladu, and Dan Alistarh. Ac/dc: Alternating compressed/decompressed training of deep neural networks. *Advances in neural information processing systems*, 34:8557–8570, 2021.
- [QLF⁺23] Zeju Qiu, Weiyang Liu, Haiwen Feng, Yuxuan Xue, Yao Feng, Zhen Liu, Dan Zhang, Adrian Weller, and Bernhard Schölkopf. Controlling text-to-image diffusion by orthogonal finetuning. *arXiv preprint arXiv:2306.07280*, 2023.
- [SA20] Sidak Pal Singh and Dan Alistarh. Woodfisher: Efficient second-order approximation for neural network compression. *Advances in Neural Information Processing Systems*, 33:18098–18109, 2020.
- [SNR21] Yi-Lin Sung, Varun Nair, and Colin A Raffel. Training neural networks with fixed sparse masks. *Advances in Neural Information Processing Systems*, 34:24193–24205, 2021.
- [SWR20] Victor Sanh, Thomas Wolf, and Alexander Rush. Movement pruning: Adaptive sparsity by fine-tuning. *Advances in Neural Information Processing Systems*, 33:20378–20389, 2020.
- [SWR⁺21] Victor Sanh, Albert Webson, Colin Raffel, Stephen H Bach, Lintang Sutawika, Zaid Alyafeai, Antoine Chaffin, Arnaud Stiegler, Teven Le Scao, Arun Raja, et al. Multitask prompted training enables zero-shot task generalization. *arXiv preprint arXiv:2110.08207*, 2021.
- [Tea23] MosaicML NLP Team. Introducing mpt-7b: A new standard for open-source, commercially usable llms, 2023. Accessed: 2023-12-22.
- [TLI⁺23] Hugo Touvron, Thibaut Lavril, Gautier Izacard, Xavier Martinet, Marie-Anne Lachaux, Timothée Lacroix, Baptiste Rozière, Naman Goyal, Eric Hambro, Faisal Azhar, et al. Llama: Open and efficient foundation language models. *arXiv preprint arXiv:2302.13971*, 2023.
- [TMS⁺23] Hugo Touvron, Louis Martin, Kevin Stone, Peter Albert, Amjad Almahairi, Yasmine Babaei, Nikolay Bashlykov, Soumya Batra, Prajwal Bhargava, Shruti Bhosale, et al. Llama 2: Open foundation and fine-tuned chat models. *arXiv preprint arXiv:2307.09288*, 2023.
- [WBZ⁺21] Jason Wei, Maarten Bosma, Vincent Y Zhao, Kelvin Guu, Adams Wei Yu, Brian Lester, Nan Du, Andrew M Dai, and Quoc V Le. Finetuned language models are zero-shot learners. *arXiv preprint arXiv:2109.01652*, 2021.
- [WGR⁰⁹] John Wright, Arvind Ganesh, Shankar Rao, Yigang Peng, and Yi Ma. Robust principal component analysis: Exact recovery of corrupted low-rank matrices via convex optimization. *Advances in neural information processing systems*, 22, 2009.
- [WKM⁺22] Yizhong Wang, Yeganeh Kordi, Swaroop Mishra, Alisa Liu, Noah A Smith, Daniel Khashabi, and Hannaneh Hajishirzi. Self-instruct: Aligning language model with self generated instructions. *arXiv preprint arXiv:2212.10560*, 2022.
- [WMA²²] Yizhong Wang, Swaroop Mishra, Pegah Alipoormolabashi, Yeganeh Kordi, Amirreza Mirzaei, Atharva Naik, Arjun Ashok, Arut Selvan Dhanasekaran, Anjana Arunkumar, David Stap, et al. Supernaturalinstructions: Generalization via declarative instructions on 1600+ nlp tasks. In *Proceedings of the 2022 Conference on Empirical Methods in Natural Language Processing*, pages 5085–5109, 2022.
- [YZY⁺18] Tao Yu, Rui Zhang, Kai Yang, Michihiro Yasunaga, Dongxu Wang, Zifan Li, James Ma, Irene Li, Qingning Yao, Shanelle Roman, et al. Spider: A large-scale human-labeled dataset for complex and cross-domain semantic parsing and text-to-sql task. *arXiv preprint arXiv:1809.08887*, 2018.
- [ZCB⁺23] Qingru Zhang, Minshuo Chen, Alexander Bukharin, Pengcheng He, Yu Cheng, Weizhu Chen, and Tuo Zhao. Adaptive budget allocation for parameter-efficient fine-tuning. *arXiv preprint arXiv:2303.10512*, 2023.
- [ZRG⁺22] Susan Zhang, Stephen Roller, Naman Goyal, Mikel Artetxe, Moya Chen, Shuhui Chen, Christopher Dewan, Mona Diab, Xian Li, Xi Victoria Lin, et al. Opt: Open pre-trained transformer language models. *arXiv preprint arXiv:2205.01068*, 2022.
- [ZXS17] Victor Zhong, Caiming Xiong, and Richard Socher. Seq2sql: Generating structured queries from natural language using reinforcement learning. *CoRR*, abs/1709.00103, 2017.

A Qualitative Results

Here we showcase some examples of the generated outputs on the GSM8k task, which includes mathematical reasoning. We consider the FFT model, as well as LoRA, SpA, and best RoSA models in the 40M budget (single epoch).

Question:

John rents his car out 10 times a month for 3 hours each time. He gets paid \$25 an hour. If his car payment is \$500, how much profit does he make on his car?

Answer (Ground Truth):

He rents his car $10*3=\ll 10*3=30\gg 30$ hour a month
 So he makes $25*30=\$ \ll 25*30=750\gg 750$ a month
 That means he has a profit of $750-500=\$ \ll 750-500=250\gg 250$ a month
 ##### 250

Answer (FFT):

He rents his car out $10*3=\ll 10*3=30\gg 30$ hours a month
 So he makes $30*25=\$ \ll 30*25=750\gg 750$ a month
 So his profit is $750-500=\$ \ll 750-500=250\gg 250$
 ##### 250

Answer (LoRA):

He makes $3*10=\$ \ll 3*10=30\gg 30$ per month
 So he makes $30*12=\$ \ll 30*12=360\gg 360$ per year
 So he makes $360-500=\$ \ll 360-500=140\gg 140$ profit
 ##### 140

Answer (SpA):

He makes $3*10=\$ \ll 3*10=30\gg 30$ per month
 So he makes $30*12=\$ \ll 30*12=360\gg 360$ per year
 So he makes a profit of $360-500=\$ \ll 360-500=140\gg 140$
 ##### 140

Answer (RoSA):

He makes $3*10=\$ \ll 3*10=30\gg 30$ per month
 So he makes $30*25=\$ \ll 30*25=750\gg 750$ per month
 So he makes $750-500=\$ \ll 750-500=250\gg 250$ per month
 ##### 250

In the above example, while both LoRA and SpA decide to calculate yearly profit, RoSA successfully solves the problem correctly.

Question:

Mary is two years younger than Joan, who is five years older than Jessa. If Jessa is 20 years old, what is the sum of the ages of the three girls?

Answer (Ground Truth):

Joan is $20 + 5 = \ll 20+5=25\gg 25$ years old.
 Mary is $25 - 2 = \ll 25-2=23\gg 23$ years old.
 Therefore, the sum of their ages is $20 + 25 + 23 = \ll 20+25+23=68\gg 68$.
 ##### 68

Answer (FFT):

Joan is $20 + 5 = \ll 20+5=25\gg 25$ years old.
 Mary is $25 - 2 = \ll 25-2=23\gg 23$ years old.
 The sum of the ages of the three girls is $23 + 20 + 25 = \ll 23+20+25=68\gg 68$ years old.
 ##### 68

Answer (LoRA):

The sum of the ages of the three girls is $20 + 5 + 2 = \ll 20+5+2=27\gg 27$ years.
 ##### 27

Answer (SpA):

Mary is $20 - 5 = \ll 20-5=15 \gg$ 15 years old.

The sum of the ages of the three girls is $20 + 15 + 15 = \ll 20+15+15=50 \gg$ 50 years.

50

Answer (RoSA):

Joan is $20 + 5 = \ll 20+5=25 \gg$ 25 years old.

Mary is $25 - 2 = \ll 25-2=23 \gg$ 23 years old.

The sum of the ages of the three girls is $23 + 20 + 20 = \ll 23+20+20=63 \gg$ 63 years.

63

While all adaptation methods (including RoSA) fail to answer the question correctly, we see that LoRA and SpA completely fail to even process it. In contrast, RoSA calculates the ages correctly and only fails to sum them up at the end.

B Singular Value Analysis on Full Fine-Tuning

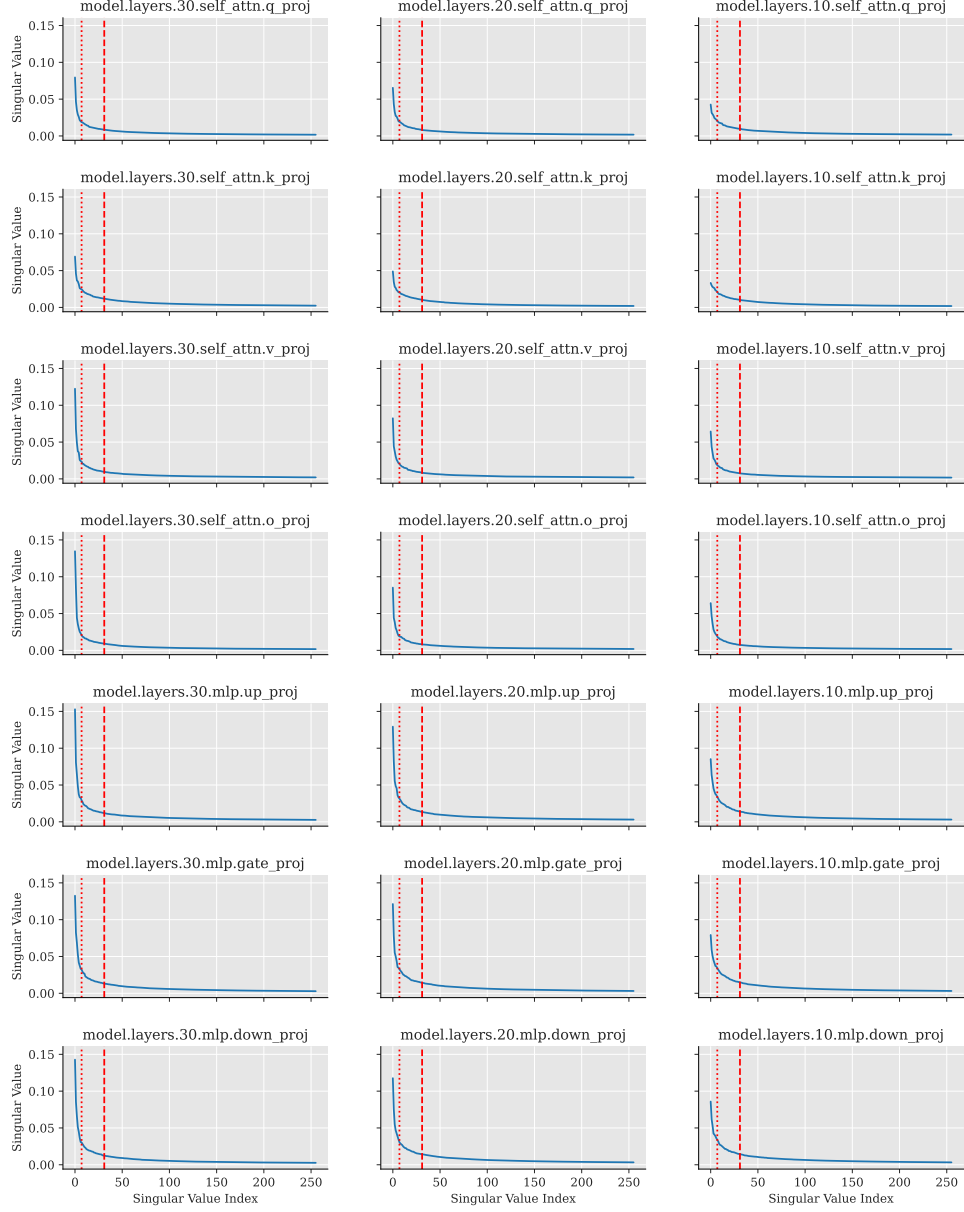


Figure 3: Sorted singular values of Δ^* for various layers of a LLaMA2-7B fully fine-tuned on GSM8k. Thresholds for ranks 8 and 32 are marked with dotted and dashed lines, respectively. The top 256 singular values are selected.

We present a straightforward analysis of the singular values obtained from Δ^* of the LLaMA2-7B model [TMS⁺23] fine-tuned on the GSM8k dataset. The focus is on a set of plots representing singular values from several randomly selected layers of the LLaMA2-7B model. The plots in Figure 3 reveal a notable pattern: a few singular values are significantly larger compared to the rest, which are relatively small yet not zero.

This pattern in the singular values suggests that the updates made during full fine-tuning of LLaMA2 exhibit a tendency towards a low-rank structure. However, they cannot be considered purely low-rank due to the presence of these small, non-zero singular values.